Penguin Huddling-inspired Energy Sharing and Formation Movement in Multi-robot Systems

Tamzidul Mina[1] and Byung-Cheol Min[2]

Abstract— Robot survivability in long term autonomous search and rescue, surveillance, monitoring operations to remote locations with minimal to no human supervision is of great importance. In such applications, a convoy of heterogeneous mobile robots in formation traveling from point A to point B on a mission, suffers from its range being constrained by the highest battery using agent. In this paper, an Emperor penguin-huddling inspired gradient based energy sharing and position shuffling scheme is proposed for heterogeneous multi-robot systems on the move, with the purpose of extending the working life of the entire convoy together. Each robot is modeled based on an Emperor penguin with carefully placed inductive coils for energy sharing with neighbors. The multi-robot system is built following the tightly packed hexagonal lattice formation for optimal charge sharing and a position coordination algorithm is proposed to allow all agents an equal opportunity to move to the center in turns which is shown to be the most advantageous position in the convoy. The convergence of the position shuffling algorithm is analyzed to show that the convoy formation is maintained over time. Simulation results validate that convoys, regardless of size, can survive and travel much further together with the proposed Emperor penguin huddling-inspired shuffling and energy sharing methods than individuals relying only on themselves.

I. INTRODUCTION

Every winter, thousands of Emperor Penguins *(Aptenodytes forsteri)* in the Antarctic survive one of the harshest environments on Earth together as a group [1]. To survive the severe cold conditions during storms and low ambient temperatures, they huddle together from several hours [2] to even days [3] depending on weather conditions as depicted in Fig. 1. This allows them to conserve and share body heat with one another; survive winds over 100mph and temperatures below -45^oC [4]. The huddles are not motionless. Penguins that are most exposed to strong winds, slowly advance along the flanks downwind to receive shelter behind the huddle [5]. This eventually causes penguins that were previously at the center to be exposed and they start to move along the flanks to the leeward side in turn as well accumulating behind the penguins that moved in before them. This flank movement and constant shuffling of the penguins in the huddle ensure that each penguin has an approximately equal opportunity for warmth and none are left behind [5].

Multi-robot systems are often proposed for long term applications of monitoring and surveillance [7], exploring

[1]Tamzidul Mina is with the SMART Lab, Department of Computer and Information Technology, Purdue University, and with the School of Mechanical Engineering, Purdue University, West Lafayette, IN 47907, USA `tmina@purdue.edu`

[2]Byung-Cheol Min is with the SMART Lab, Department of Computer and Information Technology, Purdue University, West Lafayette, IN 47907, USA `minb@purdue.edu`

Fig. 1: The huddling behavior of Emperor Penguins in winter conditions obtained from [6].

[8], search and rescue [9] etc. in remote and dangerous locations. The safety, security and survivability of these robots are important for the success of the mission. Traditionally robots have been built to be self sufficient with limited to zero access to humans [10] [11]. Regardless, each robot in the group may have a different role in the team, different hardware and movement actuation requirements; therefore use different levels of battery. Different units may even use different types/sizes of batteries altogether requiring different recharging times and processes. Regardless of having some on-board battery re-charging system (e.g. solar cells), the duration of continuous survival/work of the entire unit together is only as strong as the robot with the lowest battery life. In such instances, being able to look out for one another in a group becomes a survival requirement.

In this paper, the survival of a group of heterogeneous robots deployed on a long term mission to a remote location and on the move from site A to site B is considered. Studying the social behavior of Emperor penguins for group survival, the following concepts are proposed to ensure the survival of the entire convoy for a longer period of time in the field:

- A gradient based multi-robot charge sharing concept using carefully placed inductive coils.
- A position shuffling algorithm (PHS) for a group of robots to move to the center of the formation in turns.

II. RELATED WORK

The huddling behavior of Emperor penguins in the Antarctic has been studied extensively, but very few theoretical models have been presented so far. One theoretical model of position shuffling was presented based on observations that Emperor penguins move from the windward to the leeward side in a huddle [12]. This work was continued by taking into account models of wind flow and the temperature profile around the huddle in [13]. Their model was based on a simple rule that individual penguins relocate themselves in

the huddle to a new position where its heat loss is minimized, without displacing another. The huddle was modeled as a hexagonal grid based on [4]. Huddling modeled as a second order phase transition triggered by cold temperatures in [14]. The work was validated experimentally with a group of mice and suggested huddling as a self-organizing event relevant among large groups of endotherms such as penguins.

The term *trophallaxis* is used in entomology to describe a mutual exchange of regurgitated fluids between social insects [15]. It is also used in the multi-robot arena as exchanging information [16] or energy [17] between agents. As a solution of energy transfer between agents, a method of physical battery swapping between robots was proposed in [16]. However, the mechanism is complicated and lacks robustness for application in a heterogeneous robot group. An energy usage optimization approach for a multi-robot system inspired by the foraging behavior and energy management of honeybees was proposed in [17]. This method improves individual robot performance but fails to utilize the advantage of being in a group.

A number of wireless power transmission methods has been summarized by [18] and an efficient non-contact method using inductive coils was patented in [19]. An image processing based proper alignment of the induction coils for wireless charging between robotic agents was later proposed in [20]. The coil alignment was later improved upon with a Bayesian estimator in [21].

The work in [20] proves the feasibility of wireless charge sharing between robots. The solution proposed in this paper builds on that work by providing a bio-inspired framework for multi-robot systems where all agents receive an equal opportunity to share their charge despite heterogeneity constraints and extend the life of the convoy as a whole.
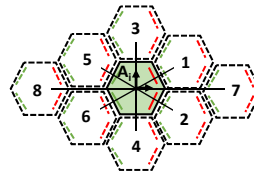
III. PROPOSED SOLUTION

Huddling of Emperor penguins involves dense packing for maximal body heat sharing and retainment as shown in Fig. 2a. In two dimensional euclidean space, the highest density lattice arrangement of circles is the hexagonal packing [22]. Therefore, we consider the hexagonal lattice formation for our proposed group of robots and note an individual's neighbors as shown in Fig. 2b following Fig. 2a.

A. Formation building block - single agent setup with Gradient based charge sharing
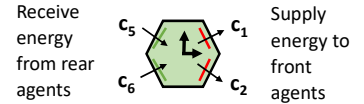
A hexagon structured robot is proposed as a concept for the charge sharing robot unit as shown in Fig. 2c. Each agent is equipped with four induction coils; two coils upfront marked in red to only transmit power to two front agents and two coils at the back marked in green to only receive power from two rear agents. Charge transfer occurs when there is a battery level difference between adjacent agents. Each side has a single coil only due to size restrictions of the robot and efficiency requirements of the charge transfer process dependent on the diameter of the coils [20]. In this study we only consider four coils rather than six on each robot to minimize energy usage in transferring energy.

Fig. 2: (a) Close packing of huddling penguins from *Nature* by PBS showing an individual A_i and its neighbors indexed $j \in (1,2,..,8)$. (b) Top view of neighboring agents modeled from (a). (c) Top view of individual agent showing inductive coil placement for energy sharing with neighbors.

Consider an agent A_i, $i \in D$ for $D = \{1,2,3,..,N\}$ with battery level b_i and its neighboring agents A_j, $j \in (1,2,..,8)$ with battery levels b_j respectively as shown in Fig. 2b. The proposed gradient based charge sharing scheme of agent A_i with surrounding agents A_j is shown in (1)-(3):

$$\Delta_{ij} = b_i - b_j, \tag{1}$$

$$f(b_i,b_j)_{\forall j \in (1,2)} = \begin{cases} K\Delta_{ij} & \Delta_{ij} > 0, \ K\Delta_{ij} \leq \Delta_t \\ \Delta_t & \Delta_{ij} > 0, \ K\Delta_{ij} > \Delta_t \\ 0 & \text{else,} \end{cases} \tag{2}$$

$$f(b_i,b_j)_{\forall j \in (5,6)} = \begin{cases} -K\Delta_{ij} & \Delta_{ij} < 0, \ -K\Delta_{ij} \geq -\Delta_t \\ -\Delta_t & \Delta_{ij} < 0, \ -K\Delta_{ij} < -\Delta_t \\ 0 & \text{else} \end{cases} \tag{3}$$

where Δ_{ij} represents the battery level gradient between agents A_i and A_j, $f(b_i,b_j)$ represents the proposed gradient based charging function with a scalar constant $K > 0$ dependent on the charging efficiency of the inductive coils subject to misalignments during charging and Δ_t is the charge sharing threshold allowed per unit time. Following Fig. 2c, the *current charge potential*, c_{A_i} of agent A_i is therefore the sum of $f(b_i,b_j)$ for $j \in (1,2,5,6)$:

$$c_{A_i} = c_5 + c_6 - c_1 - c_2 = \sum_{j \in (1,2,5,6)} f(b_i,b_j). \tag{4}$$

The proposed method allows agents to share energy in a group. Note that the charge sharing is one-directional; the net energy transfer is towards the front of the group supportive of keeping the convoy moving forward in formation. For simplicity and to maintain generality of our proposed method, each agent is assumed to be fully actuated and free to move in any direction.
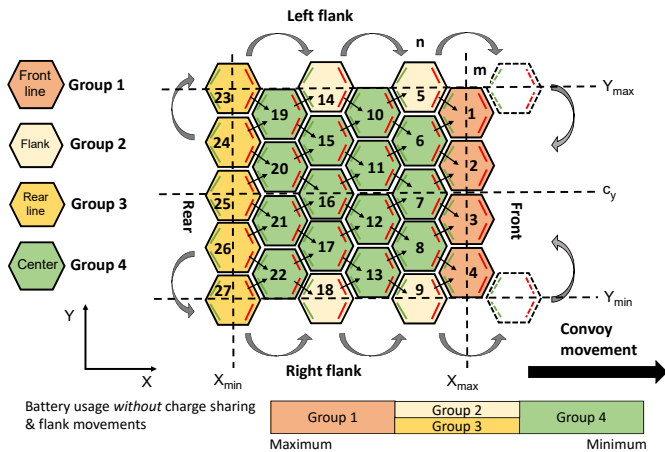
Fig. 3: m-n=4-5 formation setup for $N = 27$ agents illustrating flank movement and charge sharing. Robot groups by varying battery usage within the formation without flank movement are also identified.

B. Formation setup

We define the hexagonal lattice formation by a m-n notation with N agents each denoted as A_i, $i \in D$, where m denotes the number of agents on the front row and $n = m + 1$ denotes the number of agents on the second row from the front. This m-n structure is repeated p number of times until all N hexagonal agents are placed in a hexagonal lattice structure as shown in Fig. 3. Therefore, $p = \frac{N}{m+n}$. For simplicity, we assume that m is always even and N is a multiple of $m + n$; i.e. p is $\mathbb{Z}_{>0}$.

C. Penguin Huddling-inspired Shuffling (PHS) algorithm

Emperor penguins in a huddle lose more energy being exposed to the environment along the boundary and save energy by being at the center. Similarly, robotic agents along the boundary of a convoy use more energy monitoring the surroundings and being exposed to the environment, than robots at the center that remain protected and are able to turn off non-essential processes while following the leading agents. The battery usage with no charge sharing and no flank movement is illustrated in Fig. 3. We combine this assumption with our charge sharing scheme to present the need for the proposed position shuffling algorithm (PHS).

In Fig. 3, group 3 agents form the rear line of the convoy formation. Based on the proposed charge sharing scheme, the agents here are always providing charge to one or more agents immediately in front. This is therefore the least favorable position in the convoy. Group 2 agents form the flanks of the convoy and share charge with two adjacent agents; one providing charge and the other taking charge. However, being at the boundary the agents keep up monitoring the surroundings. This position is therefore better than group 3 but still not the best place to be in the convoy. The agents in group 1 form the front line of the convoy and they are in charge of navigation (e.g. path planning, obstacle avoidance) tasks. They have to keep their on-board functionalities on at all times. Sensing mechanisms such as laser scanners, cameras [23] use a lot of power when used continuously. Such sensors along with movement actuation results in group 1 agents having the highest battery usage in the convoy. Agents in group 4 are in the most advantageous position being at the center surrounded by agents on all directions. They are able to share charge with their neighbors most effectively, and are protected from potentially harsh environmental conditions. They can also turn off non-essential on-board tasks such as navigation, exploration, environment monitoring, etc. We will refer to this phenomenon as *center advantage*.

Even though huddles of Emperor penguins are inconsistent and change shape over time, for a robotic system, it is important to maintain a set formation for ease of control and proper functionality. If left freely to individual agents to try to move to the center directly their movements may become chaotic and inefficient. To maintain a set formation and allow agents to move to the center in turns in an organized way, the proposed one-directional charge sharing scheme creates a net power flow towards the front of the huddle. This creates an incentive for agents to try to move to the front first where they only receive charge from their neighbors. For simplicity, we assume the net movement of the entire formation is constrained to be along the x-axis only.

PHS described in Algorithm 1 systematically moves rear and flank agents to the front. The agents are attracted towards the center line c_y and hence they fill up the front line over time. The agents that were previously on the front line therefore now become center agents. As the flank agents move forward, space opens up for rear line agents to move along the flanks in turn. The previously center agents at the back therefore now become rear-line agents. This cyclic motion continues allowing all agents an equal opportunity for *center advantage*.

PHS is effective *only if* the energy saving while being at the center is more than or equal to the energy spent by an agent at the rear to move up the flank and get to the front and eventually the center; without which there is no incentive for an agent to follow Algorithm 1. This condition is formulated mathematically by:

$$
\begin{aligned}
& \mu_b^{use} z \le \mu_{ca} \Delta t_c \\
= \; & \mu_b^{use} \left(2\left\lfloor \frac{n}{2} \right\rfloor + \frac{N}{m+n} + \frac{\left\lfloor \frac{n}{2} \right\rfloor + \frac{N}{m+n}}{\left\lfloor \frac{m+n}{2} \right\rfloor} \right) \\
\le \; & \mu_{ca} \left(\left\lfloor \frac{n}{2} \right\rfloor + \frac{m}{2} \right) \left(\frac{N}{m+n} - 1 \right)
\end{aligned}
\tag{5}
$$

where z denotes the total number of movements required by an agent in the *worst case* to get from the rear line to the front, μ_b^{use} denotes the battery usage for unit movement by an agent, μ_{ca} denotes the unit *center advantage* gained by an agent per unit time by being at the center and Δt_c represents the time duration an agent is able to stay at the center from the front to the back as the formation progresses forward.

Therefore, the *minimum center advantage*, μ_{ca}^{min} required for agents to have an incentive to follow the proposed PHS

Algorithm 1 Penguin Huddling-inspired Shuffling (PHS) algorithm
---
1: **procedure** BOUNDARY MOVEMENT(X,Y,B) ▷ Position movements of agents given battery levels
2:     **Input:** Array of coordinates of agent positions, x_i and y_i, and array of corresponding battery levels, b_i.
3:     **Output:** Updated coordinate position arrays X and Y, and battery level, B
4:     Determine centerline, $c_y \leftarrow \frac{\sum_{i=0}^{N} y_i}{N}$, $Y_{max}, Y_{min}, X_{max}, X_{min}$ of formation from X,Y
5:     **for** $i = 1 \rightarrow N$ **do** ▷ Find boundary agents
6:         **if** A_i lies on $Y_{max}||Y_{min}||X_{max}||X_{min}$ **then**
7:             Determine current charge potential, c_{A_i} of A_i, setting $c_1 = c_2 = c_3 = c_4 = 1$ ▷ **Check Eq. (4)**
8:             Determine charge potential at neighboring points, $n_{cp_j} = c_{A_i}$ for $i = j$, $\forall j \in (1,2,..,8)$
9:             Determine net charge gain at neighboring points, $n_{g_{i,j}} = c_{A_i} - n_{cp_j}$, $\forall j \in (1,2,..,8)$
10:             **if** $y_i \geq c_y$ **then** ▷ if A_i is on left half
11:                 **if** $c_{A_i} \geq 0$ **then** ▷ A_i not on rear line
12:                     Check positions $j = 4,2,7$ in order, for movement availability ▷ **Refer to Fig. 2b**
13:                     **if** $n_{g_{i,j}} \geq 0$ **then**
14:                         Move A_i to *new position*
15:                 **else** ▷ A_i is on rear line
16:                     Check positions $j = 7,1,3$ in order, for movement availability ▷ **Refer to Fig. 2b**
17:                     **if** $n_{g_{i,j}} \geq 0$ && *new position* $\leq Y_{max}$ **then**
18:                       Move A_i to *new position*
19:             **else** ▷ A_i is on right half
20:                 **if** $c_{A_i} \geq 0$ **then** ▷ A_i not on rear line
21:                     Check positions $j = 3,1,7$ in order, for movement availability ▷ **Refer to Fig. 2b**
22:                     **if** $n_{g_{i,j}} \geq 0$ **then**
23:                       **if** *new position* $== 3$ **then**
24:                         Hold until front line is full and then move A_i to *new position*
25:                     **else**
26:                         Move A_i to *new position*
27:                 **else** ▷ A_i is on rear line
28:                   Check positions $j = 7,2,4$ in order, for movement availability ▷ **Refer to Fig. 2b**
29:                   **if** $n_{g_{i,j}} \geq 0$ && *new position* $\geq Y_{min}$ **then**
30:                     Move A_i to *new position*
31:         Update x_i, y_i, b_i
32:     **return** X,Y,B ▷ Return the new position coordinates and battery levels of the formation agents
---

algorithm and move to the center in turns can be written as:

$$\mu_{ca}^{min} = \frac{2\lfloor \frac{n}{2} \rfloor + \frac{N}{m+n} + \frac{\lfloor \frac{n}{2} \rfloor + \frac{N}{m+n}}{\lfloor \frac{m+n}{2} \rfloor}}{(\lfloor \frac{n}{2} \rfloor + \frac{m}{2})(\frac{N}{m+n} - 1)} \mu_b^{use}. \qquad (6)$$

The required μ_{ca}^{min} decreases with increasing N for any arbitrary m-n formation.

D. Stability analysis of proposed PHS

The m-n formation with m always even, is symmetric about the center line c_y parallel to the x-axis. The left and right flank movements happen independent of each other but are symmetric and in sync following PHS. Therefore, the stability proof of the proposed PHS algorithm is shown for the left flank only as it holds true for the right flank as well.

We denote the indices of the agents A_i, $i \in D$ in the left half of the formation as G, i.e. $G \subset D$ with elements a_i. We represent agents in G as a sequence $S(k)$ dependent on the order at which they move from the initial state defined as z_0 at time step k. At z_0 the front row agents a_i, $i \in (1,2,..,\frac{m}{2})$

denoted as H, where $(H \subset G)$, receive charge from two rear agents but do not have any agents in front to provide charge to. Following the proposed PHS algorithm, we consider one complete cycle of movement when at least one agent in H return to the front line receiving charge from two rear agents, with no one to provide charge to in front and no open space is left in the front row. Based on the sequence of movements from z_0, the boundary agents on the left flank come first in the sequence. They are followed by the rear line, and eventually the inner lines from the left-most to the middle in order. For the 4-5 formation with $N = 27$ in Fig. 3, the sequence $S(k)$ with $p(m+1)$ elements is written as:

$$S(k) = 5, 14, 23, 24, 25, 19, 20, 15, 16, 10, 11, 6, 7, 1, 2. \qquad (9)$$

We denote this initial sequence at state z_0 as S_0. The sequence $S(k)$ can be built for a general case of m-n formation with N agents and $p = \frac{N}{2m+1}$ as (7). After each cycle the sequence elements re-organize by (8) for $w = \frac{m}{2}$ following Algorithm 1. To investigate the stability of Algorithm 1, assuming that the sequence starts from S_0, we show that

$$S(k) = \begin{cases} a_e = a_0 + (e-1)d & \\ \begin{cases} a_e = a_{p-u} + v & \text{where } v \in (1,2,..,\frac{m}{2}) \\ & e \in (\alpha p+1, \alpha p+2,.., \alpha p+\frac{m}{2}) \\ a_e = a_{p-u} - m + w & \text{where } w \in (0,1,2,..,\frac{m}{2}-1) \\ & e \in (\alpha p+\frac{m}{2}+1, \alpha p+\frac{m}{2}+2,.., \alpha p+m) \end{cases} \end{cases}$$

where $a_0 = m+1$, $d = 2m+1$, $e \in (1,2,..,p)$

$\forall u \in (0,1,2,..,p-1)$, $\alpha \in (1,2,..,p)$

(7)

$$S(k+1) = \begin{cases} \begin{cases} a_1 = a(k)_{wq+1} & \\ a_e = a(k)_{vw-u} & \text{for } u \in (0,1,2,..,w-1), \\ & \forall v \in (1,2,..,q), \ e \in (2,3,..,p(m+1)) \end{cases} \\ \begin{cases} a_e = a(k)_{vw-u} & \text{for } u \in (0,1,2,..,w-1), \\ & \forall v \in (1,2,..,q), \ e \in (1,2,..,p(m+1)) \end{cases} \end{cases}$$

when $mod(N,2) = 1$, $q = \frac{p(m+1)-1}{w}$

when $mod(N,2) = 0$, $q = \frac{p(m+1)}{w}$

(8)

$S(k+s) = S(k)$ for some finite $s > 0$.

Referring to (8), the even N case shows a pattern where sets of w consecutive elements reverse order every cycle without overlap; i.e. at every even iteration, the cycle returns to the original sequence S_0. The general pattern of consecutive cycles of $S(k)$ for even N and the simplest case of $q = 1$ and arbitrary w can be written as:

$$a_i(k+1) = a_{w+1-i}(k) \qquad \forall i \in (1,2,..,w). \qquad (10)$$

The odd N case is similar to the even case of reversing sets of w consecutive elements without overlapping at each cycle. The difference is that, at each cycle the last element of $S(k)$ cycles to the front as element 1 in $S(k+1)$. Some key observations of this process include:

- At every order reversal of w consecutive elements without overlapping, element indexed $(\frac{w}{2}+1)$ in that set remains in its position; i.e. for $\beta \in (0,1,2,..,q-1)$,

$$a_{\beta w + \frac{w}{2}+1}(k+1) = a_{\beta w + \frac{w}{2}+1}(k). \qquad (11)$$

- At every cycle, a_1 and every consecutive $(w+1)^{st}$ element move forward by w; i.e. for $\beta \in (0,1,2,..,q-1)$,

$$\begin{aligned} a_{\beta w+1}(k+\beta) &\rightarrow a_{(\beta+1)w+1}(k+\beta+1) \\ a_{qw+1}(k+\beta) &\rightarrow a_1(k+\beta+1). \end{aligned} \qquad (12)$$

We denote these segments of the sequence as F_1.

- Taking (12) into account, with every order reversal of w consecutive elements without overlapping, one can see that only elements indexed $i = 2$ through $i = w$ for every set of w essentially reverse their order on every cycle; i.e. for $\beta \in (0,1,2,..,q-1)$,

$$\begin{aligned} a_{\beta w+2}, a_{\beta w+3}, a_{\beta w+4}, ..., a_{\beta w+w} \\ \rightarrow a_{\beta w+w}, a_{\beta w+w-1}, ..., a_{\beta w+3}, a_{\beta w+2}. \end{aligned} \qquad (13)$$

Following the proof for the even N case, every even iteration of (13) results in these fragments of the sequence to return to the order in S_0. Following the pattern from (12), if every $(\gamma w+1)^{st}$, $\gamma \in (0,1,2,..,q-1)$ element moves forward by w indices on every cycle and on reaching the $(qw+1)^{st}$ position cycles to index 1, these elements return to their original position after $q+1$ iterations. We denote these segments of the sequence as F_2.

Since F_1 returns to S_0 at every even iteration and F_2 returns to S_0 at every $q+1$ iterations, the number of cycles where both segments return to S_0 at the same time satisfies:

$$mod(\min_{\eta \in \{1,2\}} \eta(q+1), 2) = 0. \qquad (14)$$

Therefore, $s = \eta(q+1)$ is the number of iterations needed for $S(k+s) = S_0$ for an odd N.

For any even $m > 0$, $w = \frac{m}{2}$. For $p = 1$, the total number of agents, $N = 2m+1$ is always odd. Using (8), we get $q = 2$. The formation converges back to the original state z_0 after $s = 6$ cycles for $\eta = 2$.

For $p = g$, where g is arbitrary, the total number of agents $N = g(2m+1)$ is either odd (for odd g) or even (for even g). Using (8), we get $q = \begin{cases} \frac{2(g(m+1)-1)}{m} & \text{odd } N \\ \frac{2g(m+1)}{m} & \text{even } N \end{cases}$. For either case, q can be odd or even. Therefore, regardless of N being odd or even, the formation converges back to the original state z_0 after s cycles for the $p = g$ case depending on η.

For $p = g+1$, the total number of agents, $N = (g+1)(2m+1) = 2mg + g + 2m + 1$ is either odd(for even g) or even(for odd g). Using (8), we get $q = \begin{cases} \frac{2((g+1)(m+1)-1)}{m} & \text{odd } N \\ \frac{2(g+1)(m+1)}{m} & \text{even } N \end{cases}$. For either case, q can be odd or even. Therefore, regardless of N being odd or even, the formation converges back to the original state z_0 after s cycles for the $p = g+1$ case depending on η.

Therefore the PHS algorithm is stable for any N as it cycles agents and holds the original formation for any case of valid m, where $m > 0$, $mod(m,2) = 0$ and p, where $p = \mathbb{Z}_{>0}$ as proved by induction.

IV. VALIDATION & RESULTS

A. PHS algorithm simulation

Fig. 4 shows the sequence of unit time step position shuffling movements by agents in a 2-3 formation of $N = 10$ following Algorithm 1. After a finite number of steps, the formation returns to the initial configuration. Each agent is equipped with four induction coils; green denote receiving of charge, red denote providing of charge and inactive coils are shown in black. Agents in the most favorable positions in the convoy are marked green.
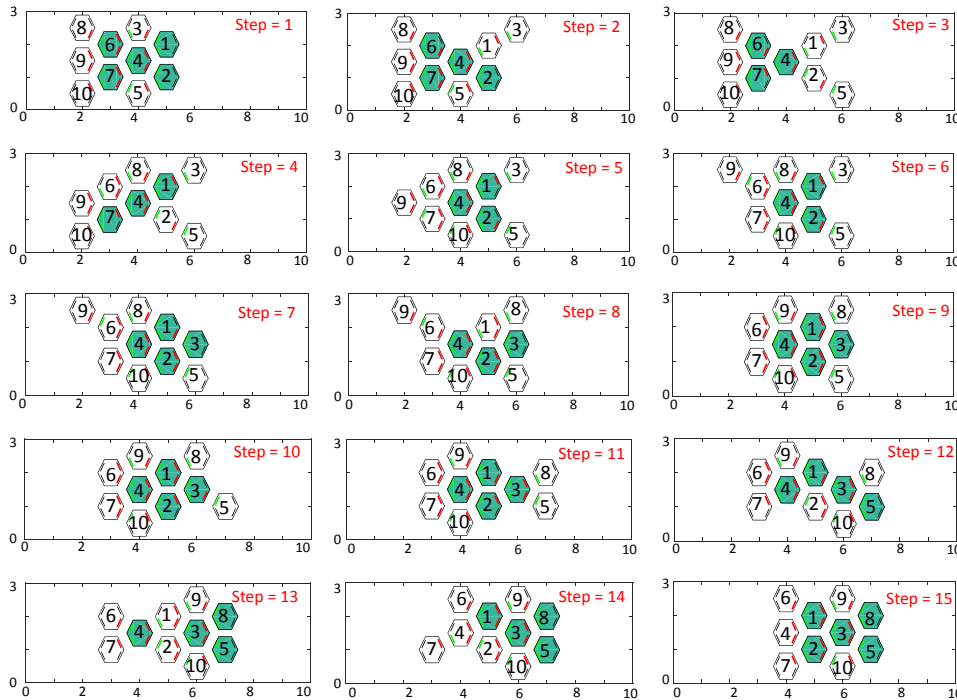
Fig. 4: Simulation snapshots showing position shuffling progression of agents and convergence back to original configuration for a 2-3 formation with $N = 10$. Agents capable of receiving charge from both rear coils are identified as green.

B. Validation setup

To validate the proposed concepts, we consider a group of N robots in the m-n formation deployed on a 2-D terrain with no obstacles; starts at an initial position A and travels along the x-axis towards B. We assume that all agents are in ideal communication with one another and are capable of making precision movements.

The convoy moves forward from point A towards point B at velocity v. The agents in the convoy are designed to be structurally identical (hexagonal) but have different roles or assigned tasks; as a result their battery usage varies significantly per unit time. The general battery usage (movement, specific tasks) is modeled per unit time as $b_{use} \sim \mathcal{N}(\mu_b^{use}, \sigma_{use}^2)$. The additional battery usage by group 1 robots per unit time using specialized navigation sensors such as LIDAR, camera etc. is modeled as $b_{ad} \sim \mathcal{N}(\mu_b^{ad}, \sigma_{ad}^2)$. The power consumption due to the charge sharing mechanism itself is assumed to be negligible compared to b_{use} based on [24]. Referring to Fig. 3, the battery usage of agent A_i, $\forall i \in D$ without charge sharing is therefore modeled as:

$$b_i = \begin{cases} b_i - b_{use} - b_{ad} & A_i \in \text{Group 1} \\ b_i - b_{use} & A_i \in \text{Group 2 \& 3} \\ b_i - b_{use} + \mu_{ca} & A_i \in \text{Group 4}. \end{cases} \quad (15)$$

C. Validation scenarios

The simulation is set up with five different scenarios, where the effectiveness of each of the proposed methods is presented individually and as combinations. At the initial state z_0, all agents start with individual batteries at 100%. In S1, the agents only move forward as a group to represent

TABLE I: Validation scenarios

Scenario	Forward movement	Center advantage	Gradient based charge sharing	Position shuffling
S1	✓			
S2	✓	✓		
S3	✓	✓		✓
S4	✓		✓	✓
S5	✓	✓	✓	✓

TABLE II: Validation parameters

Forward velocity, v	2 x-units/time
Battery usage for movement, charge sharing mechanism (groups 1, 2, 3, 4), b_{use}	$(\mu_b^{use}, \sigma_{use}^2)$ (0.5 units/time, 0.5)
Additional battery usage for navigational task (group 1), b_{ad}	$(\mu_b^{ad}, \sigma_{ad}^2)$ (0.3 units/time, 0.1)
Charge sharing threshold, $|\Delta_t|$	0.2 units/time

the conventional scenario as control. In S2, the agents are allowed the *minimum center advantage*. In S3, the agents are allowed PHS so that all agents get an opportunity for *center advantage*. In S4, PHS is allowed with gradient based charge sharing but without *center advantage* to compare the effect these two concepts have on the convoy performance. Finally, S5 utilizes all proposed concepts in this paper adopted from the huddling behavior of Emperor penguins. With this setup, the proposed concepts can be validated if the convoy travels the furthest distance in S5 compared to the other scenarios. The scenarios are summarized in Table I.

The simulation parameters are exaggerated for brevity of the simulations and are listed in Table II. We set $\mu_{ca} = \mu_{ca}^{min}$ for all cases. Since the aim of the study is to extend the working life of the convoy as a whole, the simulation stops when the battery life of *any* agent falls below 5%. The *x-distance* travelled by the convoy center and the battery level

(a) 4-5 formation, *N*=54

(b) 6-7 formation, *N*=78

(c) 10-11 formation, *N*=126
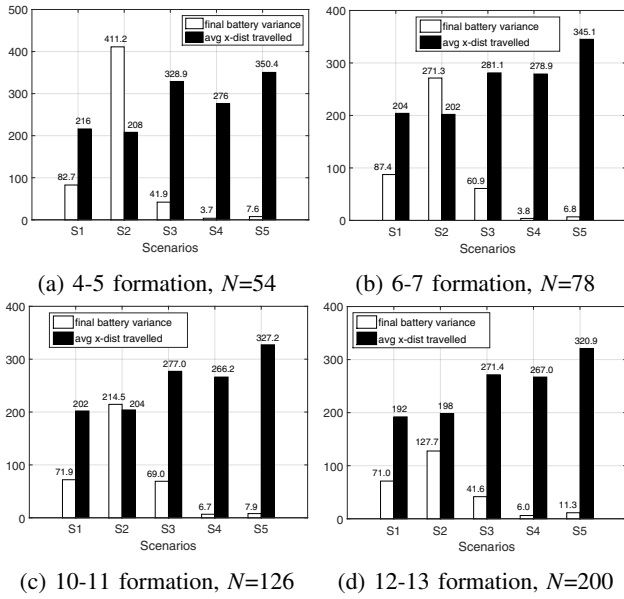

(d) 12-13 formation, *N*=200

Fig. 5: Simulation results showing the final battery level variance and *x*-distance traveled by convoys under five different scenarios. The results presented are averages of 10 simulation runs. S5 yielded the maximum *x*-distance with the lowest final battery level variance in all setups.

(a) 4-5 formation

(b) 6-7 formation

(c) 10-11 formation

(d) 12-13 formation

Fig. 6: Scenario performance comparison for m-n formation with varying *N*. S5 allows maximum *x*-distance traveled for all simulated formation cases over a wide range of *N* values.

variance amongst agents at the end are measured.

D. Validation results

A 4-5 formation of $N = 54$ robots was considered for the first set of simulations with calculated $\mu_{ca}^{min} = 0.3$. The average results from 10 independent runs for each of the scenarios are tabulated in Fig. 5a. The *x*-distance traveled by the convoy in S1 and S2 was approximately equal. This is because even though S2 allowed *center advantage*, the convoy was still as strong as the boundary agents who remained in place without any such advantage. With agents in the center saving energy, the final battery variance in S2 was significantly higher.

S1 and S4 did not allow any *center advantage*. The *x*-distance values obtained for S4 were close to S1 and S2 but consistently higher by a margin for all individual simulation runs. This observation closely relates to the final battery level variance readings for S1, S2 and S4. S4 has the lowest final battery level variance because the gradient based charge sharing method evened differences in battery levels of neighboring agents. This allowed agents using more battery to survive longer by receiving energy from its neighbors.

S3 allowed position shuffling along with S2 methods and so all robots got an equal opportunity to move to the center of the convoy in turns for *center advantage*. The convoy was no longer as strong as the boundary agents only and so the *x*-distance traveled in S3 was consistently higher than S1, S2 and S4. The final battery level variance between agents is also significantly lower than S2 but much higher than S4 without the gradient based charge sharing method.

S5 allowed the convoy to travel the maximum *x*-distance consistently with a low final battery level variance for all
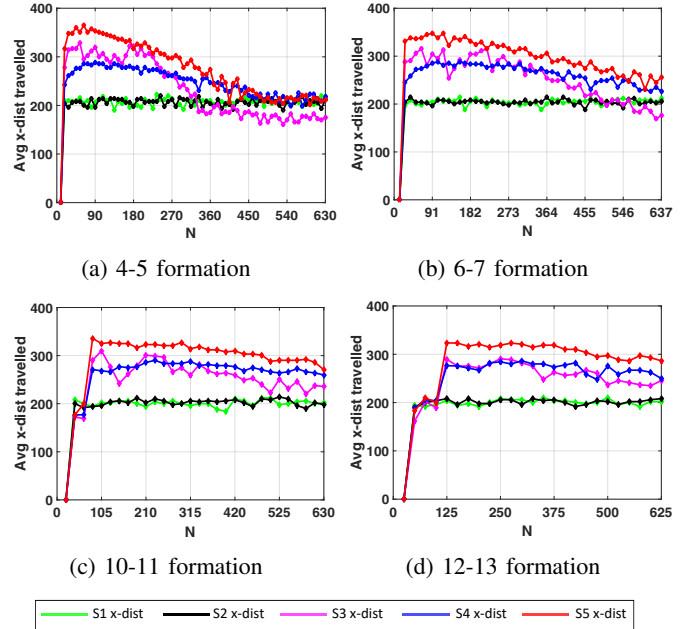
simulation runs. The combined effects of *center advantage*, PHS and the gradient based charge sharing methods allowed the convoy to survive longer in the field using the full potential of the group as validated by the simulation results.

Simulations were repeated for cases of 6-7, 10-11 and 12-13 formations with $N = 78$, 126 and 200 robots, calculated μ_{ca}^{min} of 0.225, 0.171 and 0.126 respectively. The results are shown in Fig. 5b-5d. For bigger convoys, the final battery level variance decreased for S2 as expected given the large sample size for all cases. The effect of *center advantage* was dominant over gradient based charge sharing with PHS (S3 vs S4) for smaller groups as shown by the much higher *x*-distance values obtained in the 4-5 formation with $N = 54$. The effect quickly deteriorates with bigger groups as shown for larger formation and *N* cases. However, the overall conclusion remained the same. S5 with all the proposed concepts combined, consistently yielded the best results in terms of maximum *x*-distance traveled while keeping a low variance in battery levels of agents by a wide margin.

To verify that these conclusions hold over a range of *N*, the simulations were repeated with varying *N* and corresponding μ_{ca}^{min} for all the formation cases. The 4-5, 6-7, 10-11 and 12-13 formation x-distance travelled for varying *N* are plotted in Fig. 6a-6d. In each case the average x-distance travelled over 10 independent sets of simulations for each value of *N* are used. For all m-n setups, S1 and S2 consistently yielded similar *x*-distances over the entire range of *N* as expected. S3 provided better results than S4 for smaller m-n formations with low *N*. For larger values of *N*, the *x*-distance traveled with S3 become increasingly worse. This is because the calculated μ_{ca}^{min} does not take σ_{use}^2 into account. Since for larger *N*, the agents have to move much longer distances

to get to the front, the effects of the high σ^2_{use} add up and the *center advantage* is unable to match this significant quantity of extra energy spent by any agent to get to the center. Similarly in S4, the gradient based charge sharing alone is unable to counter this effect and its performance deteriorates with increasing N as well. The performance of S5 deteriorates with larger N for the same reason but with center advantage and the gradient based charge sharing scheme working together it is able to counter the effects of the high σ^2_{use} for much larger N values than S3 or S4. Therefore, S5 shows much higher x-distances traveled by the convoy over a larger range of N compared to the other scenarios. The performance deterioration is higher in smaller formations such as the $4-5$ case where S5's performance becomes the same as S1 and S2 for $N > 500$. Therefore, we conclude that the width of the convoy (m-n) should be increased with increasing N for better performance.

V. CONCLUSION

In this paper, an Emperor penguin huddling-inspired position shuffling algorithm (PHS) and a gradient based energy sharing scheme for a multi-robot system are proposed. A hexagonal structure with carefully placed inductive coils is utilized as the unit design for charge sharing between agents. PHS allows individual robots equal opportunity to be at the center of the formation in turns. Simulation results validate that formations of different sizes successfully survive longer as a group with the proposed concepts compared to the conventional case of individuals only relying on themselves.

The improved performance by intelligent social behaviors in a multi-robot setting proposed here is the first of its type and complements autonomous missions of multi-robot search and rescue, surveillance, monitoring etc. to remote locations where self sufficiency as a group in terms of long term survivability is of great importance. Further work on adapting the proposed concepts for 3D cases with a decentralized approach for practicality and determining the optimum m-n for a given N is underway.

ACKNOWLEDGMENT

REFERENCES

[1] T. D. Williams, *The penguins: Spheniscidae*. Oxford University Press, USA, 1995, vol. 2.

[2] R. Kirkwood and G. Robertson, "The occurrence and purpose of huddling by emperor penguins during foraging trips," *Emu*, vol. 99, no. 1, pp. 40–45, 2001.

[3] J. Prévost, *Écologie du manchot empereur Aptenodytes forsteri Gray*. Hermann, 1961, vol. 1291.

[4] D. P. Zitterbart, B. Wienecke, J. P. Butler, and B. Fabry, "Coordinated movements prevent jamming in an emperor penguin huddle," *PLoS one*, vol. 6, no. 6, p. e20260, 2011.

[5] Y. Le Maho, "The emperor penguin: A strategy to live and breed in the cold: Morphology, physiology, ecology, and behavior distinguish the polar emperor penguin from other penguin species, particularly from its close relative, the king penguin," *American Scientist*, vol. 65, no. 6, pp. 680–693, 1977.

[6] C. Gilbert, S. Blanc, Y. Le Maho, and A. Ancel, "Energy saving processes in huddling emperor penguins: from experiments to theory," *Journal of Experimental Biology*, vol. 211, no. 1, pp. 1–8, 2008.

[7] D. Portugal and R. Rocha, "Msp algorithm: multi-robot patrolling based on territory allocation using balanced graph partitioning," in *Proceedings of the 2010 ACM symposium on applied computing*. ACM, 2010, pp. 1271–1276.

[8] W. Sheng, Q. Yang, J. Tan, and N. Xi, "Distributed multi-robot coordination in area exploration," *Robotics and Autonomous Systems*, vol. 54, no. 12, pp. 945–955, 2006.

[9] C. Luo, A. P. Espinosa, D. Pranantha, and A. De Gloria, "Multi-robot search and rescue team," in *Safety, Security, and Rescue Robotics (SSRR), 2011 IEEE International Symposium on*. IEEE, 2011, pp. 296–301.

[10] L. Ray, A. Price, A. Streeter, D. Denton, and J. H. Lever, "The design of a mobile robot for instrument network deployment in antarctica," in *Robotics and Automation, 2005. ICRA 2005. Proceedings of the 2005 IEEE International Conference on*. IEEE, 2005, pp. 2111–2116.

[11] L. Pedersen, D. Wettergreen, D. Apostolopoulos, C. McKay, M. DiGoia, S. Jonak, S. Heys, J. Teza, and M. Wagner, "Rover design for polar astrobiological exploration," *Robotics Institute*, p. 25, 2005.

[12] G. Stead, "Huddling behaviour of emperor penguins," *Master's thesis, University of Sheffield, United Kingdom*, 2003.

[13] A. Waters, F. Blanchette, and A. D. Kim, "Modeling huddling penguins," *PLoS One*, vol. 7, no. 11, p. e50277, 2012.

[14] M. Canals and F. Bozinovic, "Huddling behavior as critical phase transition triggered by low temperatures," *Complexity*, vol. 17, no. 1, pp. 35–43, 2011.

[15] W. Wcislo and V. Gonzalez, "Social and ecological contexts of trophallaxis in facultatively social sweat bees, megalopta genalis and m. ecuadoria (hymenoptera, halictidae)," *Insectes Sociaux*, vol. 53, no. 2, pp. 220–225, 2006.

[16] T. Schmickl and K. Crailsheim, "Trophallaxis among swarm-robots: A biologically inspired strategy for swarm robotics," in *Biomedical Robotics and Biomechatronics, 2006. BioRob 2006. The First IEEE/RAS-EMBS International Conference on*. IEEE, 2006, pp. 377–382.

[17] A. F. Arif, A. R. Ramli, K. Samsudin, and S. Hashim, "Energy management in mobile robotics system based on biologically inspired honeybees behavior," in *Computer Applications and Industrial Electronics (ICCAIE), 2011 IEEE International Conference on*. IEEE, 2011, pp. 32–35.

[18] X. Lu, P. Wang, D. Niyato, D. I. Kim, and Z. Han, "Wireless charging technologies: Fundamentals, standards, and network applications," *IEEE Communications Surveys & Tutorials*, vol. 18, no. 2, pp. 1413–1452, 2016.

[19] S. Sakoda, K. Takada, S. Suzuki, and K. Nakata, "Non-contact power transmission apparatus," Aug. 21 2012, uS Patent 8,248,027.

[20] J.-O. Kim, C.-W. Moon, and H.-S. Ahn, "Image processing based a wireless charging system with two mobile robots," in *Multimedia and Ubiquitous Engineering*. Springer, 2013, pp. 769–775.

[21] J.-O. Kim and C. Moon, "A vision-based wireless charging system for robot trophallaxis," *International Journal of Advanced Robotic Systems*, vol. 12, no. 12, p. 177, 2015.

[22] L. Fukshansky, "Revisiting the hexagonal lattice: on optimal lattice circle packing," *arXiv preprint arXiv:0911.4106*, 2009.

[23] P. Sattayasoonthorn and J. Suthakorn, "Battery management for rescue robot operation," in *Robotics and Biomimetics (ROBIO), 2016 IEEE International Conference on*. IEEE, 2016, pp. 1227–1232.

[24] L. Olvitz, D. Vinko, and T. Švedek, "Wireless power transfer for mobile phone charging device," in *MIPRO, 2012 Proceedings of the 35th International Convention*. IEEE, 2012, pp. 141–145.